

Quadratic Electro-Optic Kerr Effect: Applications to Photonic Devices

Montasir Qasymeh, Michael Cada, and Sergey A. Ponomarenko

Abstract—We propose novel applications of the quadratic electro-optic Kerr effect to photonic devices. Specifically in this work, two new illustrative examples are described, namely an electrically controlled multistable switch (ECMS), and an electrically tunable Bragg grating (ETBG). Their functionality is based on the third-order nonlinearity in an isotropic medium. On one hand, we note that the first key feature is the all-optical as well as electro-optical control/tunability. This can be achieved only in the third-order nonlinear material as opposed to a more frequently used linear electro-optic effect exploited in optical crystals. On the other hand, the second important key feature is the availability of integrated and compatible materials that show third order nonlinearity. In the first application proposed here, ECMS, the interplay between the quadratic electro-optic and all-optical Kerr effects is crucial for its tunable operation and leads to an interesting feature of storing an electrical information optically. In the second example, ETBG, employing the quadratic electro-optic effect makes it attractive thanks to the existence of the third-order nonlinearity in many interesting isotropic materials that are suitable for device integration. Devices such as modulators, switches, mixers, variable attenuators or optical limiters can be designed.

Index Terms—Integrated opto-electronics, nanocrystals, optical nonlinearities, photonic devices.

I. INTRODUCTION

PHOTONIC DEVICES utilizing nonlinear optics have been studied, designed and implemented over the last several decades. Indeed, the history of the nonlinear optics goes back as early as 1875 when Kerr [1] showed that a dc biasing electric field can induce a birefringence in optically isotropic media. The birefringence was proportional to the square of the dc electric field. This Kerr effect can be described by a third-order nonlinear susceptibility. Consequently, the following years, and especially since the sixties of the last century, have seen an extensive interest of the researchers in the possible practical exploitation of the nonlinear optical phenomena in nonlinear optical devices. Mainly the second-order and the third-order optical nonlinearities have been studied and employed.

It is known that the second-order nonlinear phenomenon that exists in various optical crystals induces the linear electro-optic effect, while the quadratic electro-optic phenomenon and the associated all-optical responses appear in third-order nonlinear

media, including isotropic materials. Many structures and devices have been proposed, designed, implemented and tested over the years. For example, the second-order nonlinearity has been exploited in electro-optic modulators [2], or for efficient second-harmonic generation [3] whereby the lithium niobate material has offered one of the best operating parameters. On the other hand, the third-order nonlinear effect has been utilized, most of the time, for all-optical switching and all-optical bistability [4], four-wave mixing or for soliton generation in optical fibers [5].

Although the use of well-known linear electro-optic materials for implementing various functional devices has been conceptually and principally successful, material problems still exist. Most optical crystals possessing strong linear electro-optic effects are not compatible with and/or suitable to device integration technologies. The scalability is also a problem and has some fundamental limitations due to, again, material and technological issues. The third-order nonlinearity, on the other hand, exists in a wide variety of commonly used materials that can be integrated and have already been used in microelectronics and for optical waveguide components. Also, all-optical effects can be utilized in device functionality, which is not the case with the linear electro-optic materials.

The problem with the third-order nonlinearity, however, is that this effect is very weak in most materials. Therefore, when a figure of merit of a device functionality is considered, the linear electro-optic materials offer superior operational parameters. The promise of the development of new materials that the material and technology researches have been focussing on in recent years is quite attractive, as it falls under the umbrella of nanotechnology. Structures, materials and devices are being developed on the nanometer scale, thus promising a potential to open a new world of scalability and integration.

Meanwhile, it is well known that reducing the size of the optical materials structures to a nanoscale (diameter smaller than the Bohr exciton in a bulk crystal of the same material) would lead to significant (orders of magnitudes) enhancements of the third-order optical susceptibility due to the confinement effect. It is thus believed that the electro-optic and all-optical devices based on the third-order nonlinearity may offer an attractive alternative solution for integrated opto-electronics. Therefore, although the challenge to design, implement and develop practical devices by building such structures based on the third-order nonlinearity appears still quite difficult, the promise exists and the potential seems to be realistic for the foreseeable future.

In this work, a different use of the third-order nonlinearity is considered. Since any third-order nonlinear medium exhibits a property of being able to support all-optical and electro-optic effects simultaneously, an interplay between the electro-optic and all-optical Kerr effects is suggested as a functional phenomena potentially exploitable in novel photonic devices. A

Manuscript received September 1, 2007; revised March 26, 2008. This work was supported in part by the Natural Science and Engineering Research Council (NSERC), Canada, in part by the National Center of Excellence (NCE) Mathematics of Information Technology and Complex Systems (MITACS) Inc., Canada, and in part by IC Litewaves Inc., Canada.

The authors are with the Electrical and Computer Engineering Department, Dalhousie University, Halifax, NS B3J 2X4, Canada (e-mail: montasir@dal.ca; michael.cada@dal.ca; serpo@dal.ca).

Color versions of one or more of the figures in this paper are available online at <http://ieeexplore.ieee.org>.

Digital Object Identifier 10.1109/JQE.2008.924430

thorough theoretical treatment is presented in [6]. It should be noted that this new interplay can only be realized with the help of a quadratic as opposed to a more frequently used linear electro-optic effect. Therefore, novel designs of electrically controlled all-optical devices can be introduced. Two illustrative examples are discussed below, namely an electrically controlled multistable switch (ECMS) and an electrically tunable Bragg grating (ETBG).

The paper is organized as follows. In Section II, the relevant theoretical background is briefly reviewed. In Sections III and IV, the proposed applications are described, including some numerical simulations. Section V addresses the critical material issues, and Section VI summarizes the results and conclusions.

II. THEORETICAL BACKGROUND

Let us consider a superposition of a dc electric field and elliptically polarized optical field, propagating along the z axis in a Kerr-like nonlinear medium. The dc field is along the x axis such that

$$E = \frac{1}{2}[a_x(E_x e^{-i\omega t} + E_{\text{ext}}) + a_y E_y e^{-i\omega t}] + \text{c.c.} \quad (1)$$

where E_x and E_y are the Cartesian components of the optical field, $a_{x,y}$ are unit vectors, and E_{ext} is the strength of the dc field. The field evolution in the medium is governed by the well known nonlinear wave equation

$$\nabla^2 E - \frac{1}{c^2} \frac{\partial^2 D}{\partial t^2} = \mu_0 \frac{\partial^2 P_{\text{NL}}}{\partial t^2}. \quad (2)$$

Here D is the electric displacement. The nonlinear polarization field P_{NL} of a Kerr-like nonlinear medium can be represented as

$$P_{\text{NL}} = \varepsilon_0 \chi^{(3)} : EEE. \quad (3)$$

Here $\chi^{(3)}$ is the third-order dielectric susceptibility.

For isotropic media whose dielectric response is of electronic origin, the third-order dielectric susceptibility tensor is known to take the form [5]

$$\chi_{ijkl}^{(3)} = \frac{1}{3} \chi_{xxxx}^{(3)} (\delta_{ij} \delta_{kl} + \delta_{ik} \delta_{jl} + \delta_{il} \delta_{jk}). \quad (4)$$

Further, we assume that ω lies well below any resonant frequency of the medium. It then follows that $\chi_{xxxx}^{(3)}$ can be considered frequency independent such that one can safely neglect nonlinear dispersion and absorption [7]. On substituting from (1) and (4) into (3), we conclude that the nonlinear polarization at frequency ω can be expressed as

$$P_{\text{NL}} = \frac{1}{2}(a_x P_x + a_y P_y) e^{-i\omega t} + \text{c.c.} \quad (5)$$

where

$$\begin{aligned} P_x &= \frac{3\varepsilon_0}{4} \chi_{xxxx}^{(3)} \left[(|E_x|^2 + \frac{2}{3}|E_y|^2) E_x \right. \\ &\quad \left. + \frac{1}{3}(E_x^* E_y) E_y + 4E_{\text{ext}}^2 E_x \right] \\ P_y &= \frac{3\varepsilon_0}{4} \chi_{xxxx}^{(3)} \left[(|E_y|^2 + \frac{2}{3}|E_x|^2) E_y \right. \\ &\quad \left. + \frac{1}{3}(E_y^* E_x) E_x + \frac{4}{3} E_{\text{ext}}^2 E_y \right]. \end{aligned}$$

In this work, we will, for the most part, restrict ourselves to the case of linearly polarized optical fields such that $E_y = 0$. Solving the nonlinear equation in (2) along with the polarization in (5) enables one to describe accurately the behavior of E using the concept of an effective nonlinear refractive index of the form

$$n_{\text{eff}}(\omega, E) = n_L(\omega) + 3\chi^{(3)} E_{\text{ext}}^2 + \frac{3\chi^{(3)} |E|^2}{4} \quad (6)$$

where $E = E_x$, $\chi^{(3)} = \chi_{xxxx}^{(3)}$, and $n_L(\omega)$ is a linear refractive index of the medium. In (6), the first two terms specify the linear and quadratic (electro-optic Kerr effect) response of the medium, whereas the last term describes the familiar all-optical Kerr nonlinear response.

III. ELECTRICALLY CONTROLLED OPTICAL MULTI STABILITY

Optical multistability occurs in systems that exhibit more than one stable optical output for a given optical input. In last decades, there was intensive interest in optical multistability as a potential functional candidate for applications in optical switching, optical communications and in optical computing. One of the first investigated structures for optical multistability was the Fabry–Pérot resonator filled with a nonlinear material. This resonator was first studied by Gibbs [8]. The optical multistability of such a system can be explained by observing the multiple outputs with the hysteresis transfer function being a consequence of unstable output ranges.

In this work, we show that such hysteresis transfer function properties are controllable by an external biasing dc electric field. This leads to the optical output stability being electrically controlled for a given optical input. A tunable all-optical device could in principle be constructed as a result. A phase operational diagram is then introduced that illustrates such a functionality; namely, that the output stability states are determined by the actual values and the history of both the electrical biasing and the optical input. In other words, optical multistability is dually (optically and electrically) controlled in a memory manner.

To demonstrate the effect, let us consider a Fabry–Pérot resonator of length L filled with a nonlinear refractive material. The cavity mirrors are assumed identical and lossless. The mirrors' reflectance, R , and transmittance, T , satisfy a standard relation, i.e., $R + T = 1$. It is straightforward to show that the transfer function between the input light intensity, I_1 , and the output light intensity, I_3 , is [7]

$$F(\gamma) = \frac{1}{1 + \frac{4R}{T^2} \sin^2(\gamma)}. \quad (7)$$

The transfer function $F(\gamma)$ is defined as $F(\gamma) = I_3/I_1$; the control parameter γ , employing the introduced concept of the effective refractive index in (6), is given by $\gamma = \gamma_0 + \gamma_{\text{ext}} E_{\text{ext}}^2 + \gamma_I I_3$, where $\gamma_0 = \phi + n_L(\omega/c)L$, $\gamma_{\text{ext}} = n_{\text{NL EXT}}(\omega/c)L$, and $\gamma_I = n_{\text{NL}}(\omega/Tc)L$. Here 2ϕ is the phase of the mirrors' reflectivity; $n_{\text{NL}} = 3\chi^{(3)}/4\varepsilon_0 c n_L^2$, and $n_{\text{NL EXT}} = 3\chi^{(3)}/8n_L$.

As can be seen from the transfer function in (7), the biasing dc electric field controls the hysteresis of the resonator; this is a direct consequence of the interplay between the quadratic electro-optic and self-phase modulation effects. In Fig. 1, the input-output intensity relation is shown, using a nonlinear material with $\chi^{(3)} = -9 \times 10^{-16} \text{ m}^2 \text{V}^{-2}$. Each hysteresis loop in the figure corresponds to a different dc bias. The biasing dc fields are $E_{\text{ext}1} = 0$, $E_{\text{ext}2} = 5.9 \text{ V}/\mu\text{m}$, $E_{\text{ext}3} = 7 \text{ V}/\mu\text{m}$,

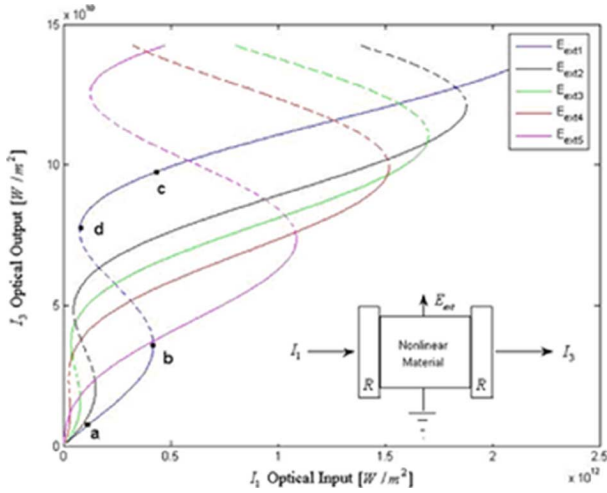


Fig. 1. Input–output characteristic for different biasing dc electric fields.

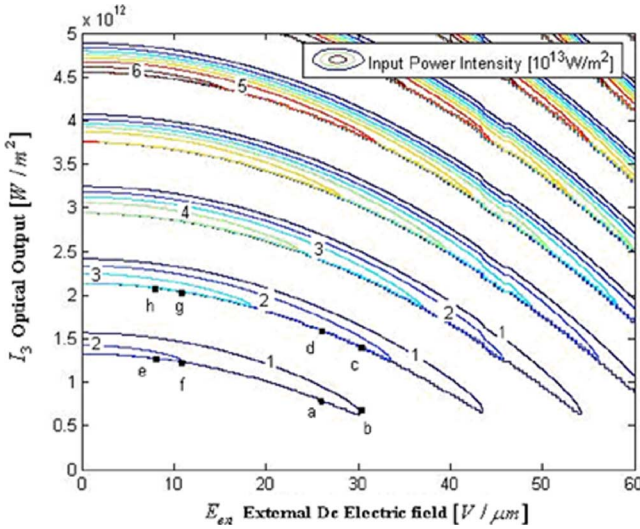


Fig. 2. Optical output as a function of the biasing dc electric field for different optical inputs.

$E_{\text{ext}4} = 8 \text{ V}/\mu\text{m}$, and $E_{\text{ext}5} = 10 \text{ V}/\mu\text{m}$. The dashed lines are the unstable optical outputs for given dc electric fields that cause the multistabilities. For example, on applying the external dc field $E_{\text{ext}1}$ and increasing the input intensity, the output intensity will increase until it jumps from point b to point c . On decreasing the optical input from there on, the optical output would jump back from point d to a . These transition bistable values are, however, quite different for different biases. It is thus clearly seen in Fig. 1 that the dc electric field controls the required optical input for bistable switching as well as the corresponding output values. It could be noted that, for example, some outputs, which are unstable, become stable, and vice versa, for different biases. This tuning property offers a promise for designing novel electrically tunable/reconfigurable all-optical devices.

An interesting question arises whether and how the system evolution will change if the biasing dc field is a control parameter while the optical input remains constant. To answer this question, one can employ the linear stability analysis [9] that will describe the output stability behavior depending on the dc bias. We now consider the situation such that all characteristic evolution times, including the cavity round-trip, and the cavity

decay time are much longer than a typical time, associated with the dynamics of the control parameter γ . Therefore, the time response of the system is characterized by a single response time of this control parameter, and the control parameter evolution is governed by the following phenomenological rate equation [10]

$$\begin{aligned} \tau \frac{\partial \gamma}{\partial t} &= -(\gamma - \gamma_0 - \gamma_{\text{ext}} E_{\text{ext}}^2 - \gamma_I I_3) \\ &= \gamma_I I_1 F(\gamma) - \gamma + \gamma_0 + \gamma_{\text{ext}} E_{\text{ext}}^2. \end{aligned} \quad (8)$$

Here τ is a relaxation time. Note that the response time is equal to zero at the equilibrium value $\bar{\gamma} = \gamma_I I_1 F(\bar{\gamma}) + \gamma_0 + \gamma_{\text{ext}} E_{\text{ext}}^2$.

Now, let us perturb the control parameter γ from its equilibrium value $\bar{\gamma}$ by $\gamma = \bar{\gamma} + \Delta\gamma$. The time response to a small perturbation can be described by the following differential equation:

$$\tau \frac{\partial (\Delta\gamma)}{\partial t} + \left[1 - I_1 \gamma_I \frac{\partial F(\gamma)}{\partial \gamma} \right] (\Delta\gamma) = 0. \quad (9)$$

The solution for such a small perturbation can be obtained straightforwardly from (9) as

$$\Delta\gamma(t) = c_0 e^{-(1 - I_1 \gamma_I (\partial F(\gamma)/\partial \gamma))t/\tau} \quad (10)$$

where c_0 is a constant.

It follows that all stable optical outputs can be realized provided that

$$\frac{\partial F}{\partial \gamma} < \frac{F}{\gamma_I I_3}. \quad (11)$$

One can now construct a phase diagram of all possible stable optical outputs for a given input as a function of the external dc electric field. Fig. 2 maps the entire possible stable optical outputs space as a function of the external dc electric field with different optical inputs being a parameter. It can be concluded from Fig. 2 that the dependence of the system evolution on the external dc field exhibits a hysteresis-like character as well. Namely, the value of the optical output, at a certain dc field, depends on the history of that dc field. For example, considering a given optical input $I_1 = 10 \text{ W}/\mu\text{m}^2$, starting from the initial point a , and having the optical output $I_3 \simeq 0.75 \text{ W}/\mu\text{m}^2$, increasing the dc biasing field will drive the operating point to follow the arc $a \rightarrow b$. Further increase of the dc biasing field will cause the operating point to jump from position b to position c , where $I_3 \simeq 1.4 \text{ W}/\mu\text{m}^2$. It follows that on decreasing the external dc field to the same initial value one can cause the operating point to shift to position d , where $I_3 \simeq 1.6 \text{ W}/\mu\text{m}^2$.

Such an optically stored electric hysteresis control is a novel feature that can be potentially utilized in the future applications. For example, this hysteresis effect can be used to store electrical signal (information) optically since the optical system here can remember and store the action of the past electrical signal behavior. For efficient optical electric signal's storage, i.e., low electric signal amplitude, one can use higher optical input. Furthermore, a dc electrical offset can be employed. For example, in Fig. 2, by using optical input $I_1 = 20 \text{ W}/\mu\text{m}^2$, and a dc offset of $8 \text{ V}/\mu\text{m}$ to bias the initial operating point at point e , an electrical signal with amplitude less than $3 \text{ V}/\mu\text{m}$ can be stored optically by changing the optical output from the point e to the point h while passing through the arc $e \rightarrow f \rightarrow g \rightarrow h$. This will change the optical output from $I_3 \simeq 1.3 \text{ W}/\mu\text{m}^2$ to $I_3 \simeq 2.2 \text{ W}/\mu\text{m}^2$ while the electrical signal is not there

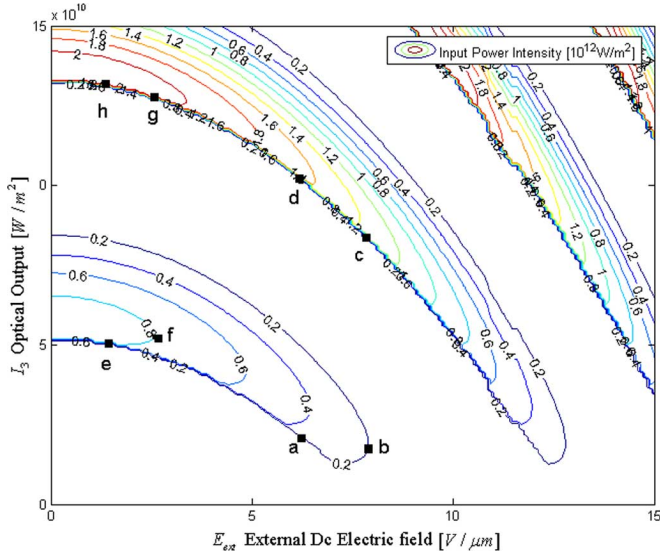


Fig. 3. Optical output as a function of the biasing dc electric field for different optical inputs.

any more, i.e., **optical storage of an electrical signal** has been achieved.

One can obviously expect to have more efficient hysteresis behavior, both electrical and optical, by employing materials with stronger nonlinearity. For example, in order to examine the behavior in more detail, Fig. 3 maps the entire possible stable optical outputs space as a function of the external dc electric field with different optical inputs being a parameter, in analogy to Fig. 2. The third-order nonlinear susceptibility was taken as $\chi^{(3)} = -9 \times 10^{-15} \text{ m}^2 \text{ V}^{-2}$.

It is seen in Fig. 3, that in order to observe the dual hysteresis behavior, the needed optical inputs and the electrical bias are smaller than in Fig. 2. In comparison, using an optical input $I_1 = 0.8 \text{ W}/\mu\text{m}^2$ and a dc offset of $2 \text{ V}/\mu\text{m}$ to bias the initial operating point at the point *e*, an electrical signal with amplitude less than $1.5 \text{ V}/\mu\text{m}$ can be stored optically by changing the optical output from the point *e* to the point *h* while passing through the arc $e \rightarrow f \rightarrow g \rightarrow h$. This will be changing the optical output from $I_3 \simeq 0.05 \text{ W}/\mu\text{m}^2$ to $I_3 \simeq 0.13 \text{ W}/\mu\text{m}^2$. Thus, the optical system remembers the electrical signal efficiently.

IV. TUNABLE BRAGG GRATING

Bragg gratings have a variety of applications in optical communications, e.g., as filters, gain flatteners, and dispersion compensators [11]. They also find use in other fields such as medical applications [12] or civil structures [13]. Controlling (tuning) the dispersion relation and thus the photonic (Bragg) bandgap electronically offers a new free parameter for the system designer and, as a result, enhances the system flexibility for the implementation of new functionalities.

An electronically tunable Bragg grating (TBG) can be constructed based on the third-order nonlinearity discussed here. The potential of the external electric field assistance in the third-order nonlinearity becomes apparent when it is instrumental to the functionality of the Bragg grating structure. The key feature is the well-known dispersion property of Bragg gratings

whereby their dispersive response is very strong if one operates sufficiently close to the Bragg resonance [14]. This takes place even when the refractive index changes are very small.

A simple analytical model below demonstrates the effect of the external electric field on one-dimensional periodically layered medium. Let us assume a medium with a periodic refractive index of the form

$$n_L(z) = n_L(z + l\Lambda) \quad (12)$$

where n_L is the linear refractive index, Λ is the period, and l is an integer. One can approximate the structure's reflectivity by [14]

$$R = \frac{\kappa^* \kappa \sinh^2(sL)}{s^2 \cosh^2(sL) + (\Delta B)^2 \sinh^2(sL)}. \quad (13)$$

Here L is the length of the periodic media, κ is the linear coupling coefficient, and the parameter s is given by $s^2 = \kappa^* \kappa - (\Delta B)^2$, where ΔB is the phase mismatch factor. The bandwidth of the main reflectivity peak (the bandwidth of the transmittance forbidden frequency zone) can then be approximated by

$$\Delta\omega_{\text{gap}} = \frac{2c}{\bar{n}} |\kappa| \quad (14)$$

with \bar{n} being the geometrical average of the linear refractive index, and c being the speed of light in vacuum.

Assuming now low light intensity such that one can neglect the all-optical effects, and applying a dc electric field in the direction of the optical field polarization, (13) and (14) can be used. The effective refractive index concept, introduced by (6), can also be employed with the last all-optical term there being omitted. Taking the periodic layered media that has the following refractive index distribution:

$$n_L(z) = \begin{cases} n_{L1} & : 0 < z < \frac{1}{2}\Lambda \\ n_{L2} & : \frac{1}{2}\Lambda < z < \Lambda \end{cases}. \quad (17)$$

The effect of the biasing dc field can be described by exploiting (13) and (14). The corresponding parameters can be expressed as

$$\begin{aligned} \bar{n} &= \left(\frac{(n_{L1} + 3\chi_1^{(3)} E_{\text{ext}}^2)^2}{2} + \frac{(n_{L2} + 3\chi_2^{(3)} E_{\text{ext}}^2)^2}{2} \right)^{1/2} \\ \kappa &= -\frac{i}{\lambda \bar{n}} [(n_{L1} + 3\chi_1^{(3)} E_{\text{ext}}^2)^2 - (n_{L2} + 3\chi_2^{(3)} E_{\text{ext}}^2)^2] \\ \Delta B &= \frac{\omega_0}{c} \bar{n} - \frac{\pi}{\Lambda}. \end{aligned} \quad (18)$$

Here $\chi_{1,2}^{(3)}$ is the nonlinear susceptibility of the first and the second layer materials, respectively, and λ is the light wavelength. If one considers a special case such that the nonlinear susceptibility of the second material's layer is very small, the parameters in (18) can be simplified as

$$\begin{aligned} \bar{n} &= \frac{1}{\sqrt{2}} (n_{L1}^2 + n_{L2}^2 + 6\chi_1^{(3)} E_{\text{ext}}^2 n_{L1})^{1/2} \\ \kappa &= -\frac{i}{\lambda \bar{n}} (n_{L1}^2 - n_{L2}^2 + 6\chi_1^{(3)} E_{\text{ext}}^2 n_{L1}) \\ \Delta B &= \frac{\omega_0}{c} \bar{n} - \frac{\pi}{\Lambda}. \end{aligned} \quad (19)$$

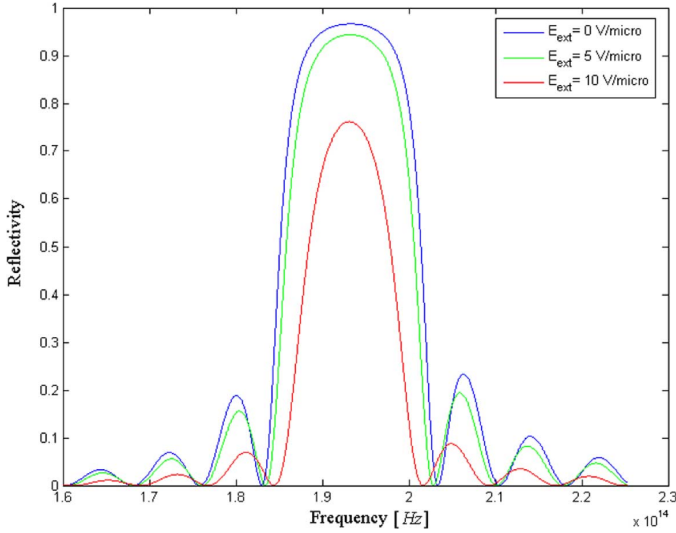


Fig. 4. Bragg reflectivity with different biasing dc electric fields.

Fig. 4 shows the reflectivity of a periodic layered media of two materials, which has the Bragg frequency equal to 193 THz. One of the materials is assumed to have $\chi^{(3)} \approx 10^{-16} \text{ m}^2/\text{V}^2$, while the other material is linear.

One can see from the figure that the external dc electric field controls the reflectivity's amplitude and the lower and upper cut-offs of the band edges. In this illustrative case, the reflectivity peak value changes from 0.95 to 0.75 by changing the dc electric field from 0 to 10 V/ μm . At the same time, each band edge of the main bandgap is shifted by 2.7357 THz. One notices that it is the band edge shift that is quite pronounced.

In Fig. 5 the silicon nanocrystal with $\chi^{(3)} \approx 2.6 \times 10^{-17} \text{ m}^2/\text{V}^2$ is employed as the first material. The Bragg lower edge frequency lies at 1065 nm. Here the other material has a negligible nonlinear susceptibility. In this case, the reflectivity peak value changes from 1 to 0.98 by changing the dc electric field from 0 V/ μm to 10 V/ μm . At the same time, each band edge of the main bandgap is shifted by 1.7764 THz. One should note that, as stated before, the potential of the external electric field assistance in the third-order nonlinearity becomes apparent in the Bragg grating structure, if one operates it sufficiently close to the Bragg resonance.

On the other hand, as a very conservative example, let us consider one of the layered materials be ordinary glass with an extremely small nonlinearity of $\chi^{(3)} \approx 2.381 \cdot 10^{-22} \text{ m}^2/\text{V}^2$, and the other material be air. A change in the dc bias from 0 V/ μm to 10 V/ μm will have no noticeable effect on reflectivity's peak amplitude. However, the main band edges will shift by 10 MHz, which is certainly a measurable value even at optical frequencies and thus potentially usable in new devices.

This type of a tunable Bragg grating with characteristics illustrated in Figs. 4 and 5 suggests possible novel applications. For example, an opto-electronic amplitude modulator or an electrically controlled switch can be designed. Also, a fast electronic mixer or an electrically controlled pulse shaper for short optical pulses with carrier frequency close to the band edge appears feasible, or a variable electrically controlled optical attenuator or a limiter are realistic and very attractive. The grating material could be any of the known material systems that are suitable

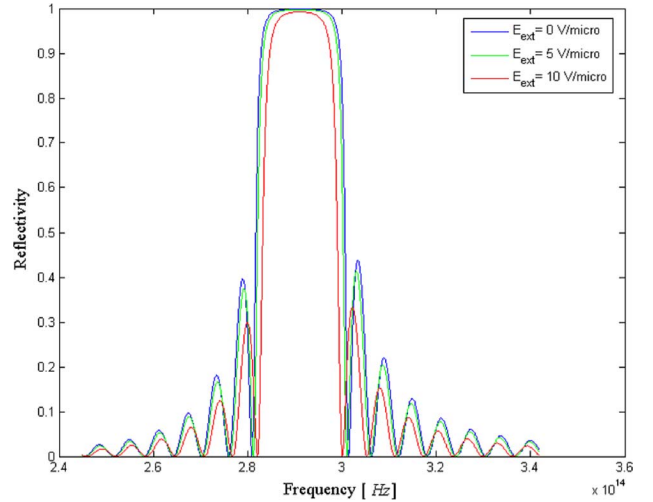


Fig. 5. Bragg reflectivity with different biasing dc electric fields (silicon-nanocrystal).

for monolithic integration and possesses the third-order nonlinearity, including glass, III-V or II-VI compound semiconductors, organic materials, or low-dimension structures, to mention just a few examples. Moreover, using the high index-contrast periodic structures (photonic crystals) in two or three dimensions certainly appear very appealing considering the added electrical control the Kerr medium offers.

V. MATERIALS

A material with a large enough third-order optical nonlinearity still represents a fundamental challenge to implementing efficient photonic devices based on nonlinear optics. One of the lately most studied techniques to enhance the nonlinearity is a low-dimensional structured material. The nonlinear response of the low-dimensional materials has been theoretically and extensively experimentally investigated [14]–[30]. Most of the research attention has been directed towards the resonant active nonlinearity regime that results from exciton states, where the incident light contains frequencies close to or slightly above the fundamental absorption edge. The enhancement of the excitonic binding energy caused by the quantum confinement effect in such structures can lead to drastic increases in the third-order optical nonlinearity.

However, employing a dc electric field requires the off-resonance nonlinearity regime that results from the anharmonic motion of bound electrons, where the light frequencies are well below the absorption edge and within the transparency region. Therefore, our search for a suitable medium should be directed towards a nonlinear material in its transparency regions, which is possessing a large nonlinearity.

Fortunately, it has been reported theoretically [21] and experimentally [22]–[25] that the three-dimensional quantum confinement can enhance and control the nonlinear optical properties in the transparency region. For example in [22], a nonresonant nonlinearity of the photoluminescent 75% porosity *p*-type microporous silicon is reported at photon wavelengths spanning the middle-gap region of the sample. The reported nonlinear susceptibility values were $\chi^{(3)} = 6.2 \times 10^{-17} \text{ m}^2/\text{V}^2$ at $\lambda = 1064 \text{ nm}$, $\chi^{(3)} = 2.68 \times 10^{-17} \text{ m}^2/\text{V}^2$ at 900 nm, and

$\chi^{(3)} = 1.17 \times 10^{-16} \text{ m}^2/\text{V}^2$ at 860 nm, respectively. The experimental results revealed no evidence of two-photon absorption, which means that the nonlinearity values were all refractive. Another experimental work of characterizing high-porosity freestanding porous silicon sample can be found in [23], where the nonlinear refractive index values, signs and the pure refraction nature in the transparent region all agreed with the above reported values. Another important experiment is reported in [24], where the measured third-order optical nonlinear refraction of nanostructure silica nanoaerogels was quite large compared to that of bulk silica, with a value of $\chi^{(3)} = 10^{-17} \text{ m}^2/\text{V}^2$. A high figure of merit, $\chi^{(3)}/\beta\lambda$, was observed for $0.07 \text{ g}/\text{cm}^3$ density with $\beta = 2 \times 10^{-10} \text{ m}/\text{W}$. ZnO nanoparticles coated by surfactant molecules were synthesized by microemulsion method in the experiment reported in [25]. The third-order optical nonlinearity of ZnO composite nanoparticles with different interfacial chemical environment were investigated. The sign and the magnitude of the real part of $\chi^{(3)}$ and the nonlinear absorption coefficient, β , at 790 nm were measured as $n_{\text{NL}} = -5.2 \times 10^{-16} \text{ m}^2/\text{W}$ and $\beta = 1.16 \times 10^{-10} \text{ m}/\text{W}$, respectively, for ZnO-DBS composite nanoparticles with DBS being the anionic surfactant, dodecyl benzene sulfonate. The values for ZnO-CTAB composite nanoparticles with CTAB being the cationic surfactant, cetyltrimethyl ammonium bromide, were $n_{\text{NL}} = -2.2 \times 10^{-17} \text{ m}^2/\text{W}$ and $\beta = 4.5 \times 10^{-12} \text{ m}/\text{W}$, respectively. The ultrafast nonlinear response time ($\sim 250 \text{ fs}$) measured by the time-resolved pump-probe technique at an excitation wavelength of 647 nm suggests that the optical nonlinearity below the bandgap originated mainly from a rapid electronic polarization process or a virtual process such as the optical Stark effect.

Another important low-dimensional material for nonlinear optics is the organic molecules material. It can be processed easily into a stable solid-state material, and it is flexible in terms of molecular design. Several interesting experimental results have been reported for such materials. For example, an experimental measurement of a nano-optical material based on the nonconjugated conductive polymer, poly (β -pinene) doped with iodine has been reported in [26], that showed a large third-order nonlinearity at $\lambda = 0.633 \mu\text{m}$. The value of $\chi^{(3)} = 0.58 \times 10^{-16} \text{ m}^2/\text{V}^2$ was, at its maximum, about 50 times larger than that of nitrobenzene. Also, experimental observations of a large third-order optical nonlinearity in the fullerene containing polyurethane films at $\lambda = 1.55 \mu\text{m}$ have been reported in [27] with $n_{\text{NL}} = 2 \times 10^{-16} \text{ m}^2/\text{W}$. An interesting property of this material is that it has a zero nonlinear absorption coefficient at $\lambda = 1.55 \mu\text{m}$, thus a large figure of merit is obtained.

Another important material is the semiconductor quantum-dot array embedded in an organic medium [28]. For organic-CdS nanocomposites, large two-photon absorption in the visible and near infrared regions are experienced when the CdS nanoparticles have relatively large particle sizes, about 3 nm or larger, yet still within the limits of confinement requirements [29]. For smaller particles, the exciton bands are shifted toward the blue, and the nonlinear response in the visible and near infrared regions, away from resonance, is expected to be mostly real. An experimental measurement of a cadmium sulfide-dendrimer nanocomposite with nanoparticle sizes of 2.2 nm has been reported in [30]. Large nonlinear coefficients and low nonlinear absorption losses were observed at $\lambda = 1064 \text{ nm}$. The nonlinear susceptibility was

$\chi^{(3)} = 10^{-17} \text{ m}^2/\text{V}^2$ and the nonlinear absorption coefficient was $\beta = 5 \times 10^{-13} \text{ m}/\text{W}$.

Although, as briefly outlined above, a significant progress has been made to synthesize and produce a relevant material with a sufficiently large third-order nonlinearity, indeed, further research is still needed. Availability of applicable materials with large nonlinearities and low losses at suitable operating wavelengths is an ongoing challenge that, clearly, keeps many interesting device designs, including some parts of the proposals in this work, within a conceptual rather than practical domain.

VI. CONCLUSION

The applicability of a biasing dc electric field in third-order optical nonlinear media to photonic devices has been discussed and modeled. Two illustrative novel applications based on this quadratic electro-optic Kerr effect have been proposed. First, electrically controlled optical multi-stability has been investigated whereby it was found that the biasing dc electric field can control the optical multi-stability transfer function. It was also shown that the electrical controllability offers memory-type functionality where the value of the optical output, at a certain dc field, depends on the history of that dc field. Thus, an attractive way of storing electrically encoded information is envisaged via a state of the optical field. Second, a simple tunable Bragg grating has been analyzed. A modulator/switch, a fast opto-electronic mixer, a variable attenuator, or an optical limiter could be designed exploiting such a dispersive structure or a similar configuration (interferometer, resonator etc.).

Since the third-order nonlinearity exists in many materials suitable for photonic devices and their integration, the exploitation of the quadratic Kerr effect offers ultra-fast functionalities and opens up new possibilities (isotropic materials, integration, scalability, cost) that cannot be otherwise realized with commonly used linear electro-optic materials. Also, since the off-resonant nonlinear response of many optical media well below the saturation point is Kerr-like, the presented results are applicable to a wide variety of photonic materials and they may offer viable alternatives for future generations of efficient opto-electronic devices, components and systems.

REFERENCES

- [1] J. Kerr, *Phil. Mag. J. Sci.*, ser. 4th, vol. 50, pp. 337–393, Nov. 1875.
- [2] E. L. Wooten, K. M. Kissa, A. Yi-Yan, E. J. Murphy, D. A. Lafaw, P. F. Hallemeier, D. Maak, D. V. Attanasio, D. J. Fritz, G. J. McBrien, and D. E. Bossi, "A review of lithium niobate modulators for fiber-optic communications systems," *IEEE J. Sel. Topics Quantum Electron.*, vol. 6, no. 1, pp. 69–82, Jan./Feb. 2000.
- [3] M. M. Fejer, "Nonlinear optical frequency conversion," *Physics Today*, vol. 47, no. 5, pp. 25–32, 1994.
- [4] M. Cada, "Nonlinear optical devices," *Opt. Pura Aplicada*, vol. 38, no. 3, pp. 1–11, 2005.
- [5] G. P. Agrawal, *Nonlinear Fiber Optics*, 4th ed. San Diego, CA: Academic, 2007.
- [6] M. Cada, M. Qasymeh, and J. Pistora, "Electrically and optically controlled cross-polarized wave conversion," *Opt. Exp.*, vol. 16, no. 5, pp. 3083–3100, Mar. 2008.
- [7] R. W. Boyd, *Nonlinear Optics*, 2nd ed. Amsterdam, The Netherlands: Academic, 2003.
- [8] H. M. Gibbs, S. L. McCall, and A. V. Venkatesan, "Differential gain and bistability using a sodium-filled Fabry-Pérot interferometer," *Phys. Rev. Lett.*, vol. 36, p. 1135, 1976.
- [9] H. M. Gibbs, *Optical Bistability: Controlling Light With Light*. London: Academic Press, 1985.

- [10] J. A. Goldstone and E. M. Garmire, "Macroscopic manifestations of microscopic optical bistability," *J. Opt. Soc. Amer. B*, vol. 1, p. 466, 1984.
- [11] N. M. Litchinitser, B. J. Eggleton, and G. P. Agrawal, "Dispersion of cascaded fiber grating in WDM light wave systems," *J. Lightw. Technol.*, vol. 16, no. 8, pp. 1523–1529, Aug. 1998.
- [12] N. E. Fishery, J. Surowiecy, D. J. Webby, D. A. Jacksony, L. R. Gavrilovz, J. W. Handz, L. Zhangx, and I. Bennionx, "In-fiber Bragg gratings for ultrasonic applications," *Meas. Sci. Technol.*, vol. 8, pp. 1050–1054, 1997.
- [13] Y. B. Lin, K. C. Chang, J. C. Chen, and T. K. Lin, "Applications of fiber Bragg grating sensors in civil structures," in *Proc. 3rd Taiwan-Japan Workshop Lifeline Performance Disaster Mitigation*, 2004, pp. 72–75.
- [14] A. Yariv and P. Yeh, *Optical Waves in Crystal*. New York: Wiley, 1984.
- [15] B. I. Greene, J. Orenstein, R. R. Millard, and L. R. Williams, "Non-linear optical response of excitons confined to one dimension," *Phys. Rev. Lett.*, vol. 58, no. 26, pp. 2750–2753, 1987.
- [16] E. Hanamura, "Very large optical nonlinearity of semiconductor microcrystallites," *Phys. Rev. B*, vol. 37, no. 3, pp. 1273–1279, 1988.
- [17] R. Chen, D. L. Lin, and B. Mendoza, "Enhancement of third-order nonlinear optical susceptibility in Si quantum wires," *Phys. Rev. B*, vol. 48, no. 16, pp. 11879–11882, 1993.
- [18] S. Ohtsuka, T. Koyama, K. Tsunetomo, H. Nadata, and S. Tanaka, "Nonlinear optical properties of CdTe microcrystallites doped glasses fabricated by laser evaporation method," *Appl. Phys. Lett.*, vol. 61, no. 25, pp. 2953–2954, 1992.
- [19] Y. P. Rakovich, M. V. Artemyev, A. G. Rolo, M. I. Vasilevskiy, and M. J. M. Gomes, "Third-order optical nonlinearities in thin films of CdS nanocrystals," *Phys. Stat. Sol. (b)*, vol. 224, no. 1, pp. 319–324, 2001.
- [20] J. Loicq, Y. Ronette, J.-L. Delplanche, and Y. Lion, "Non-linear optical measurements and crystalline characterization of CdTe nanoparticles produced by the 'electropulse' technique," *New J. Phys.*, vol. 6, no. 32, pp. 1–13, 2004.
- [21] Y. Haseba, H. Kiluchi, T. Nagamura, and T. Kajiyama, "Large electro-optic Kerr effect in nanostructured Chiral liquid crystal composites over a wide temperature range," *Adv. Mater.*, vol. 17, no. 19, pp. 2311–2315, 2005.
- [22] D. Cotter, M. G. Burt, and R. J. Manning, "Below-band-gap third-order optical nonlinearity of nanometer-size semiconductor crystallites," *Phys. Rev. Lett.*, vol. 68, p. 1200, 1992.
- [23] S. Lettieri and P. Maddalena, "Nonresonant Kerr effect in microporous silicon: Nonbulk dispersive behavior of below bandgap $x^{(3)}(\omega)$," *J. Appl. Phys.*, vol. 91, p. 5564, 2002.
- [24] S. Lettieri, P. Maddalena, L. P. Odierna, and D. Ninno, "Measurements of the nonlinear refractive index of freestanding porous silicon layers at different wavelengths," *Philosoph. Mag. B*, vol. 81, no. 2, pp. 133–139, 2001.
- [25] J. T. Seo, S. M. Ma, K. Lee, H. Brown, A. Jackson, T. Skyles, N. M. Cubbage, B. Tabibi, K. P. Yoo, S. Y. Kim, S. S. Jung, and M. Namkung, "Highly porous silica nanoaerogels for ultrafast nonlinear optical applications," *Key Eng. Mater.*, vol. 287, pp. 352–356, 2005.
- [26] R. Wang, X. Wu, B. Zou, L. Wang, S. Xie, J. Xu, and W. Huang, "Non-resonant optical nonlinearity of ZnO composite nanoparticles with different interfacial chemical environments," *Mat. Res. Innovat.*, vol. 2, pp. 49–52, 1998.
- [27] H. Rajagopalan, P. Vipra, and M. Thakur, "Quadratic electro-optic effect in a nano-optical material based on the nonconjugated conductive polymer, poly (β -pinene)," *Appl. Phys. Lett.*, vol. 88, no. 3, pp. 033109–033112, 2006.
- [28] Q. Chen, L. Kuang, E. H. Sargent, and Z. Y. Wang, "Ultrafast nonresonant third-order optical nonlinearity of fullerene-containing polyurethane films at telecommunication wavelengths," *Appl. Phys. Lett.*, vol. 83, no. 11, pp. 2115–2117, 2003.
- [29] Y. Gao, N. Q. Huong, J. L. Birman, and M. J. Potasek, "Large nonlinear optical properties of semiconductor quantum dot arrays embedded in an aorganic medium," *J. Appl. Phys.*, vol. 96, no. 9, pp. 4839–4842, 2004.
- [30] Y. Gao, N. Q. Huong, J. L. Birman, and M. J. Potasek, "Highly effective thin film optical filter constructed of semiconductor quantum dot 3-D arrays in an organic host," *Proc. SPIE*, vol. 5592, p. 272, 2005.
- [31] M. Etienne, A. Biney, A. D. Walser, R. Dorsinville, D. L. V. Bauer, and V. Balogh-Nair, "Third-order nonlinear optical properties of a cadmium sulfide-dendrimer nanocomposite," *Appl. Phys. Lett.*, vol. 87, p. 181913, 2005.



Montasir Qasymeh received the B.S. degree in electrical engineering from Mutah University, Jordan, in 2003, the M.S. degree in optical communication and photonic technologies, from Politecnico di Torino, Turin, Italy, in 2005. He is currently working toward the Ph.D. degree in electrical engineering at Dalhousie University, Halifax, NS, Canada.

His current research interests are focusing in nonlinear optics including electro-optic and all optical devices.



Michael Cada graduated from the Czech Technical University, Prague, in 1976, as an electrical engineer. He pursued the Ph.D. degree in optoelectronics at the Academy of Sciences of Czechoslovakia, Prague, while finishing his research work in the Physics Institute of A. N. Lebedev, Moscow, Russia, in the laboratory of Nobel Prize Laureate A.M. Prokhorov (1979).

He has published over 70 scientific papers, over 70 industrial research reports, and over 70 conference papers. He worked in the research laboratories of Nortel Networks, Ottawa, ON, Canada, Siemens AG, Munich, Germany, and Telecom Italia, Torino, Italy. He was an Invited Professor at Ecole Polytechnique Federal of Lausanne, Switzerland, Polytechnique University of Madrid, Spain, and Polytechnique University of Valencia, Spain. He was a Canada Research Chair in Integrated Active Photonics at University of Ottawa, Canada. He is currently with Dalhousie University, Halifax, NS, Canada, where he is Professor of electrical engineering and a Director of the Photonics Applications Laboratory. Over the years, he has supervised a number of very successful graduate students who found high positions in industry, universities and government laboratories around the world. His deep knowledge and insight in optical waveguides and electromagnetic problems, combined with his experimental experience, related to photonic device design have been a sought-after expertise valuable to various industries and institutions. He has attracted substantial amounts of research funds in support of his activities.



Sergey A. Ponomarenko received the diploma in physics from Novosibirsk State University, Novosibirsk, Russia, in 1994, and the Ph.D. degree in theoretical optical physics from the Department of Physics and Astronomy, University of Rochester, Rochester, NY, in 2002.

His work toward his degree and later research as a Postdoctoral Associate (2002–2004) was supervised by E. Wolf, a founding father of optical coherence theory. In 2004, he accepted a prestigious Director's Postdoctoral Fellowship at Los Alamos National Laboratory where he worked as a Director's Postdoctoral Fellow until July of 2006. In July 2006, he joined the Faculty of the Department of Electrical and Computer Engineering, Dalhousie University, Halifax, NS, Canada as a Canada Research Chair (Tier II). He published 35 scientific papers in peer-reviewed journals and 1 technical report. His research interests are in the general areas of nonlinear optics and quantum optics.